Report No. KS-25-01 ▪ FINAL REPORT ▪ October 2025

Non-Cantilever Fatigue Remaining-Life Simulation Software Using Probabilistic Wind Model for All Counties in Kansas

Khalid W. Al Shboul, Ph.D.
Hayder A. Rasheed, Ph.D., P.E.

Kansas State University Transportation Center

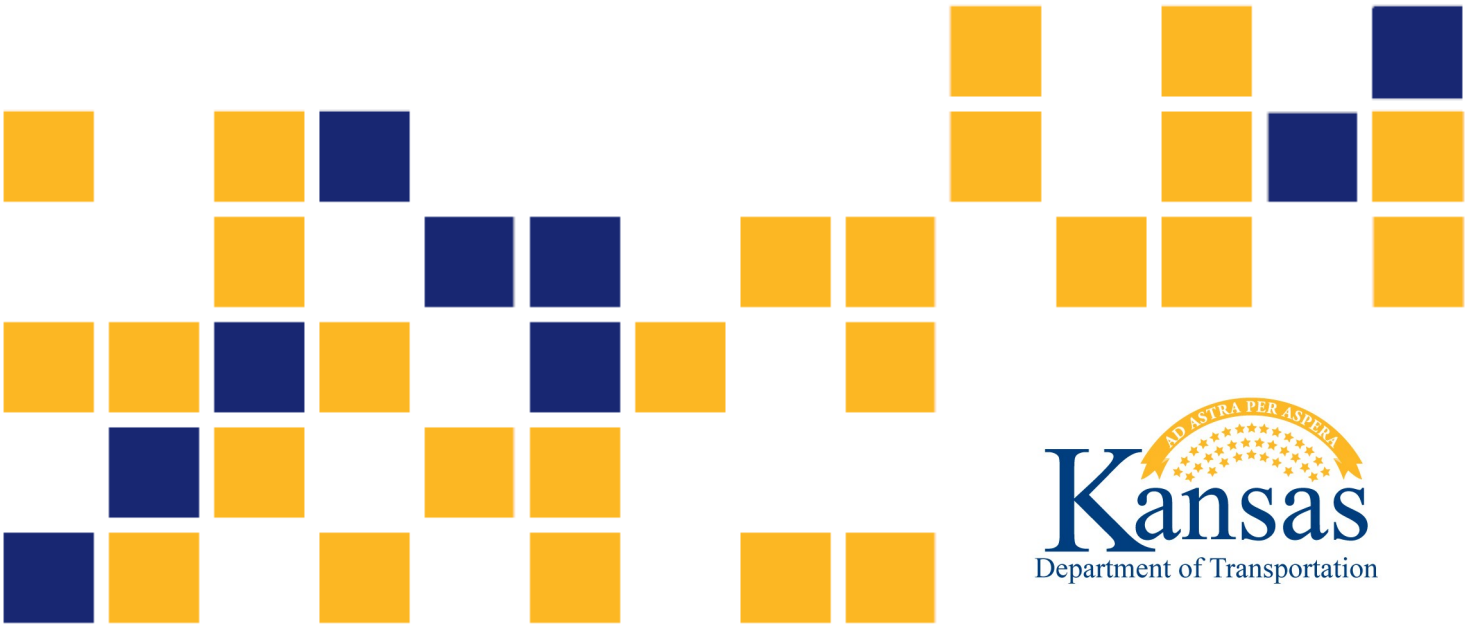

Kansas
Department of Transportation

1 Report No. KS-25-01	**2 Government Accession No.**	**3 Recipient Catalog No.**
4 Title and Subtitle Non-Cantilever Fatigue Remaining-Life Simulation Software Using Probabilistic Wind Model for All Counties in Kansas		**5 Report Date** October 2025 **6 Performing Organization Code**
7 Author(s) Khalid W. Al Shboul, Ph.D.; Hayder A. Rasheed, Ph.D., P.E.		**8 Performing Organization Report No.**
9 Performing Organization Name and Address Kansas State University Transportation Center Department of Civil Engineering 2118 Fiedler Hall 1701C Platt Street Manhattan, KS 66506-5000		**10 Work Unit No. (TRAIS)** **11 Contract or Grant No.** C2197
12 Sponsoring Agency Name and Address Kansas Department of Transportation Bureau of Research 2300 SW Van Buren Topeka, Kansas 66611-1195		**13 Type of Report and Period Covered** Final Report October 2021 – September 2022 **14 Sponsoring Agency Code** RE-0849-01

15 Supplementary Notes
For more information write to address in block 9.

16 Abstract

This study presents a comprehensive tool to accurately predict the remaining fatigue life of full-span overhead highway sign support structures subjected to a long and sustained wind fluctuation. Synthetic wind time-histories were developed by superimposing cosine waves over frequencies of 3–300 Hz and randomly generated phase angles. The Kaimal spectrum was utilized to build a database of wind time histories for each daily mean wind speed in Kansas over a period of 45 years. Moreover, each wind time history was modified to capture the mean speed and high speed each day, and then the rainflow counting technique was used to extract the relationship of the wind speed versus the cycle number for a given time span from the synthetic wind time-history. Fatigue evaluations were conducted using axial truss members. Potential fatigue failure was assessed for each structural member after the stress range was amplified using an average dynamic amplification factor. Miner's rule was used to estimate the fatigue life of the sign structure, and a computationally affordable simulation package was developed to generate wind time-histories, cycle counting, structural modeling, and fatigue life calculations. This package was used to evaluate the fatigue life of a non-cantilever sign structure in Wichita, Kansas, and predict the end-of-fatigue-life of two members in this structure. Accordingly, inspections of these members revealed the existence of unnoticed severe fatigue cracks, while other members did not show any signs of distress.

17 Key Words Fatigue Failure, Mechanical Fatigue, Fatigue Cracking, Traffic Signs		**18 Distribution Statement** No restrictions. This document is available to the public through the National Technical Information Service www.ntis.gov.	
19 Security Classification (of this report) Unclassified	**20 Security Classification (of this page)** Unclassified	**21 No. of pages** 35	**22 Price**

Form DOT F 1700.7 (8-72)

This page intentionally left blank.

Non-Cantilever Fatigue Remaining-Life Simulation Software Using Probabilistic Wind Model for All Counties in Kansas

Final Report

Prepared by

Khalid W. Al Shboul, Ph.D.
Hayder A. Rasheed, Ph.D., P.E.

Kansas State University Transportation Center

A Report on Research Sponsored by

THE KANSAS DEPARTMENT OF TRANSPORTATION
TOPEKA, KANSAS

and

KANSAS STATE UNIVERSITY TRANSPORTATION CENTER
MANHATTAN, KANSAS

October 2025

NOTICE

The authors and the state of Kansas do not endorse products or manufacturers. Trade and manufacturers names appear herein solely because they are considered essential to the object of this report.

This information is available in alternative accessible formats. To obtain an alternative format, contact the Office of Public Affairs, Kansas Department of Transportation, 700 SW Harrison, 2nd Floor – West Wing, Topeka, Kansas 66603-3745 or phone (785) 296-3585 (Voice) (TDD).

DISCLAIMER

The contents of this report reflect the views of the authors who are responsible for the facts and accuracy of the data presented herein. The contents do not necessarily reflect the views or the policies of the state of Kansas. This report does not constitute a standard, specification or regulation.

Abstract

This study presents a comprehensive tool to accurately predict the remaining fatigue life of full-span overhead highway sign support structures subjected to a long and sustained wind fluctuation. Synthetic wind time-histories were developed by superimposing cosine waves over frequencies of 3–300 Hz and randomly generated phase angles. The Kaimal spectrum was utilized to build a database of wind time histories for each daily mean wind speed in Kansas over a period of 45 years. Moreover, each wind time history was modified to capture the mean speed and high speed each day, and then the rainflow counting technique was used to extract the relationship of the wind speed versus the cycle number for a given time span from the synthetic wind time-history. Fatigue evaluations were conducted using axial truss members. Potential fatigue failure was assessed for each structural member after the stress range was amplified using an average dynamic amplification factor. Miner's rule was used to estimate the fatigue life of the sign structure, and a computationally affordable simulation package was developed to generate wind time-histories, cycle counting, structural modeling, and fatigue life calculations. This package was used to evaluate the fatigue life of a non-cantilever sign structure in Wichita, Kansas, and predict the end-of-fatigue-life of two members in this structure. Accordingly, inspections of these members revealed the existence of unnoticed severe fatigue cracks, while other members did not show any signs of distress.

Acknowledgments

This research was made possible by funding from the Kansas Department of Transportation's (KDOT) Kansas Transportation Research and New-Developments (K-TRAN) Research Program. Thanks are extended to the KDOT team members in the Bureau of Structures and Geotechnical Services who supported the project during all its development stages. Special thanks are extended to Karen Peterson, Eric Anderson, and Mark Hurt.

Table of Contents

List of Tables

List of Figures

Chapter 1: Introduction

1.1 Overview

Full-span overhead sign support structures are critical ancillary systems that help guide drivers via a set of mounted highway signs. Cantilever and butterfly structures are also commonly utilized along major highways throughout the United States. Functionally, highway sign structures must support large truss spans so roadway users can acquire essential highway information and be alerted to possible hazards without sign obstructions in the travel path. Due to their long spans and their utilization of hollow circular tubes with a relatively small mass, these structures are semi-rigid with a low natural frequency and damping ratio (Arabi et al., 2018; Kacin et al., 2010; Li et al., 2005). As a result, they experience fatigue failure due to various fatigue loading scenarios, such as natural wind gust, galloping, vortex shedding, and truck-induced vibrations (Hosch & Fouad, 2010).

1.2 Objectives

Full-span overhead sign support structures are critical ancillary systems that use a set of mounted highway signs to guide drivers. The Kansas Department of Transportation (KDOT) also utilizes cantilevered and butterfly structures in their transportation system. A frequent comprehensive evaluation of full-span overhead sign support structures is essential to prevent possible hazards that may result from fatigue damage. However, the inspection accuracy of these structures depends on accurate quantification of wind-loading scenarios that structures may experience during their lifetimes. Therefore, this project sought to develop a detailed spatial wind-speed interpolation using finite element shape functions to provide wind-speed records for all counties in Kansas and derive daily wind-time profiles for a 45-year period (1975–2019). Another objective was to conduct rainflow analysis of the time histories to describe a wind-loading scenario in terms of the number of cycles. Overall, this study intended to ensure the resulting wind-speed data set is projectable into the future by mirroring the data about end of December 2019 / beginning of January 2020 timeline.

1.3 Scope

This report includes a total of five chapters. The first chapter provides a general introduction to the project, and the second chapter presents a brief literature review relevant to topics addressed by this report. Chapter 3 includes a detailed formulation of the finite element modeling of the structures. Chapter 4 describes the results and discusses the finding of the analyses, while Chapter 5 draws necessary conclusions and presents recommendations.

Chapter 2: Literature Review

Highway sign structures must be routinely and effectively inspected to ensure continued functionality of the signs and driver safety. A thorough investigation should include every structure member as well as routine fatigue inspections to verify structural integrity. However, many state highway agencies avoid these cumbersome, costly, and time-consuming investigations; thereby, increasing the potential for unnoticed fatigue cracking and potential catastrophic failures. To ensure that support structures are proportioned to withstand all wind-induced loading scenarios and that wind-induced stresses are below the constant amplitude fatigue threshold (CAFT), AASHTO 2013 specifications (AASHTO, 2015) require support structures to be designed for fatigue via nominal stress-based classifications of typical connection details or experiment-based methodologies.

Previous studies have provided reasonably detailed methods of quantifying fatigue damage in highway sign structures, and many researchers have performed fatigue simulations using various wind-loading scenarios, structure types, and analysis methods (Chen et al., 2001; Creamer et al., 1979; DeSantis & Haig, 1996; Dexter & Ricker, 2002; Fouad & Hosch, 2011; Hong et al., 2016; Letchford & Cruzado, 2008). For example, Ginal (2003) used ANSYS to investigate the fatigue performance of three full-span overhead sign support structures with natural wind load and truck-induced pressures. Results showed that truck-induced pressure caused minimal damage to most full-span overhead sign structures, while natural wind loading (20–50 mph) caused the most damage, resulting in a predicted remaining structural life of 4–27 years.

Kacin et al. (2010) used stress histories from the finite element solution to conduct a fatigue analysis of pristine and damaged overhead four-chord truss sign structures to identify critical structural members. They used the Kaimal wind spectrum for base wind speeds of 5–25 mph. Although they predicted infinite fatigue life for the welded diagonal members, they recommended field monitoring of the real structure and accurate field measuring of the wind loading to confirm exact structural conditions. Although wind is dynamic in nature, as a structural loading, research has shown that its effect could be represented as mean speed plus fluctuating speeds (Cochran, 2012). However, wind recording stations typically report average speeds instead of instantaneous

wind speeds, so for practical engineering applications, the fluctuating wind spectrum is usually simulated using the Davenport spectrum (Davenport, 1962) or the Kaimal spectrum (Kaimal et al., 1972).

The primary objective of the current study was to build a comprehensive tool to accurately predict the remaining fatigue life of full-span overhead highway sign support structures subjected to long and sustained wind fluctuations. Synthetic wind time-histories were developed by adapting the Kaimal power spectral density function of naturally occurring winds (Kaimal et al., 1972) to build a wind time-history dataset for each daily mean wind speed over a period of 45 years in Kansas. Moreover, each time history was modified to capture the mean speed and high speed each day, and then the relationship between wind speed and the number of cycles was extracted from the synthetic wind time history using the rainflow counting technique. Fatigue evaluations were conducted using axial member stresses corresponding to each wind speed in the ensemble and hundreds of structural simulations. Potential fatigue failure was assessed for each structural member after the stress range was amplified using an average dynamic amplification factor (DAF). These assessments evaluated the ratio of consumed fatigue cycles to ultimate fatigue cycles using Miner's rule to estimate the fatigue life.

Chapter 3: Formulation

3.1 Overhead Sign Structure Model and Automation

This study used Staad Pro V8i SS6 (Bentley Systems, 2016) to model various overhead sign structures and perform first-order static analysis. The number of simulations directly corresponded to the number of times the wind speeds varied in the chosen period. Nodes and members were built using model generator C# code written for this purpose. Aluminum members were modeled using a 2-node frame element, and the upper and lower chord members were modeled as continuous members, while their intermediate nodes were connected to secondary members as pinned connections, as shown in Figure 3.1. Furthermore, upper and lower chord members were rigidly connected to the columns with appropriate offsets. The material used was 6061 aluminum alloy with modulus of elasticity of 68.9 GPa. The base supports were completely fixed because the base plate contained four corner anchor bolts.

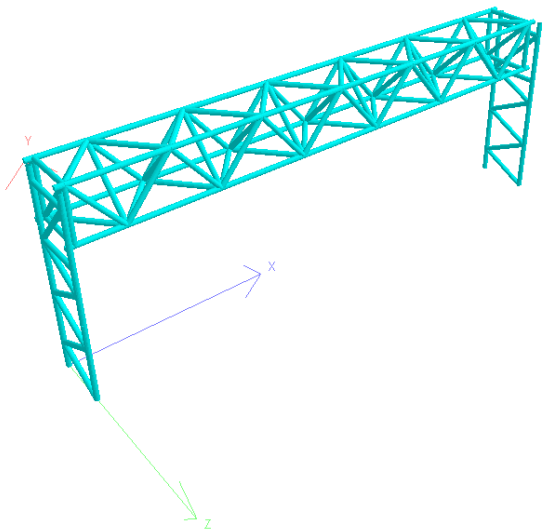

Figure 3.1: Model of Four-Chord Box Truss

3.2 Model Automation

A user-friendly software was written and programmed using the object-oriented programming language C# to model the four-chord box structures in Staad Pro (Figure 3.2). The

software can generate Staad Pro-based structural models easily and quickly for any structure with unique geometry. The input parameters required for modeling are panel size, number of panels, truss offsets, member thicknesses, sign dimensions, and wind speed. This software is vital for structural modeling and for simulating wind pressure at any wind speed by applying it to the signs and normal structural members or members that are transverse to the plane of the sign.

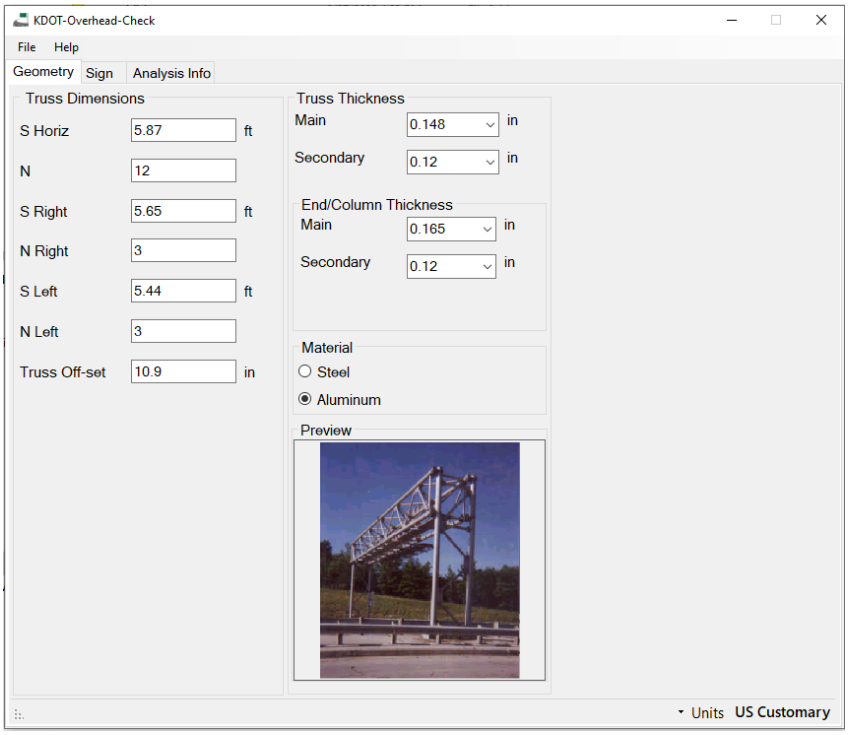

Figure 3.2: Modeler Interface

3.3 Dynamic Amplification Factor (DAF)

This study performed the static analysis for a structural model and then amplified the generated stresses using an overall blanket average (DAF) to account for the dynamic nature of the wind load. The average DAF was calculated assuming harmonic excitations, as in Equation 3.1, which requires calculation of the frequency-response curve for the range of frequencies used in the wind spectrum generation [3–300 HZ], as shown in Figure 3.3.

$$DAF = \frac{\int_0^{1.4} \frac{dR}{\sqrt{(1-R^2)^2 + (2\xi R)^2}}}{1.4}$$

Equation 3.1

Where ξ is the damping ratio and R = $\frac{\omega}{\omega_n}$ ω: the excitation frequency, ω_n: natural frequency of the structure

The average DAF was calculated in Equation 3.1 by integrating the area under the curve across an excitation ratio of (0–1.4), where the value of the DAF exceeds unity.

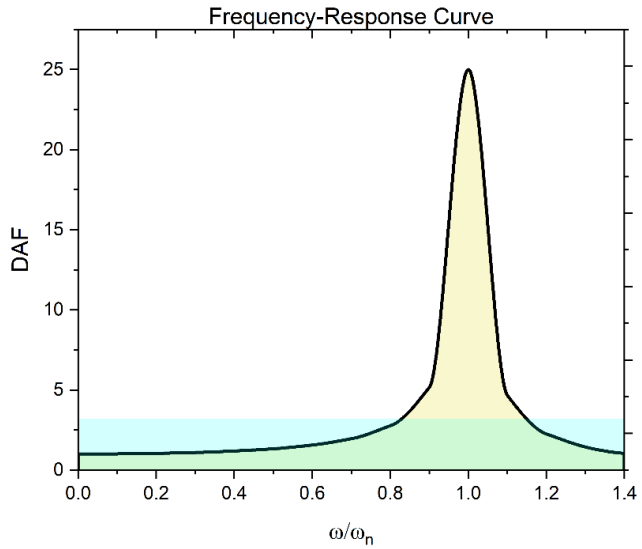

Figure 3.3: Frequency-Response Curve and Average DAF ($\xi = 0.02$)

3.4 Structural Wind Loading

Alshareef et al. (2022) developed and reported wind speed records for counties and cities in Kansas. The developed software was used to simulate the effect of natural wind by specifying a certain wind speed. The software generated and populated the wind loading to the Staad Pro models. The effects of wind loading on both signs and members were considered. First, wind pressure was calculated using the following expression (AASHTO, 2015):

$$Pz = 0.00256K_z GV^2 I_r C_d \ (psf)$$

Equation 3.2

Where K_z is the height and exposure factor based on the height of the member from Equation 3.3, G is the gust factor of 1.14, V is the applied wind velocity (mph), and I_r is the importance factor of 1.0.

$$Kz = 2.01(\frac{Z}{Z_g})^{\frac{2}{\alpha}}$$

Equation 3.3

Where Z is the height above the ground at which the pressure is calculated, Z_g = 274.3 m (900 ft.), α = 9.5

The drag coefficient (C_d) was based on the object size and shape. For truss members, the value of C_d was 1.2, and for the signs, the value of C_d was based on the aspect ratio (width/height). After generating the pressure from each wind speed in the timespan under investigation, the pressure was converted to force by multiplying it by the gross area over which the pressure was applied.

3.5 Fatigue Analysis and Life Prediction

3.5.1 S-N Curve Implementation

The stress-life method was used in this research to evaluate the fatigue life of various structural elements. AASHTO (2015) provides *S-N* curves for different connection types based on a wide range of laboratory fatigue tests of full-scale structures. However, an experimental *S-N* curve for the welded aluminum was used to determine the number of cycles to failure at each stress value on the member level using Equation 3.4.

$$N_i = (\frac{\sigma_i}{A})^{\frac{1}{B}}$$

Equation 3.4

Where N_i is the number of cycles to failure at *i-th* stress range, σ_i is the member stress value corresponding to a wind speed value, and A and B are constants to be determined from a log-log plot of the *S-N* curve.

The relationship of the stress amplitude to the number of cycles to failure for the welded aluminum from Sonsino (2007) is plotted on a log-log scale in Figure 3.4 to find the values of A and B.

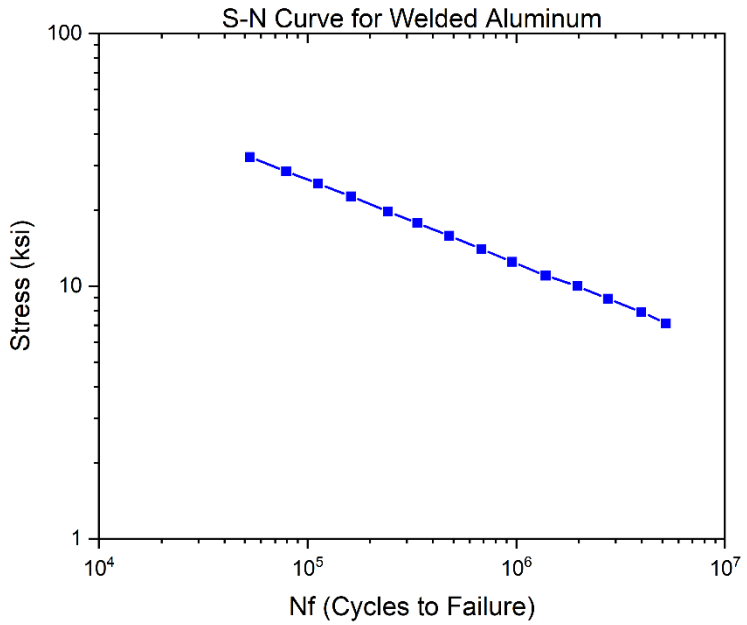

Figure 3.4: S-N Curve for Welded Aluminum
Source: adapted from Sonsino (2007)

The S-N curve was extrapolated to extend to lower stress values to cover a broad range of stresses that may affect overhead structures if the aluminum does not have a threshold stress. The plotted data in Figure 3.4 appear to fall along a straight line, meaning Equation 3.4 can calculate A and B values from two points along the curve.

3.5.2 Rainflow Counting and Palmgren-Miner Rule

Wind time histories generated for the 45 years of data demonstrated highly irregular variations of speed with time. The rainflow counting technique, developed by Matsuishi and Endo (1968), was adapted to convert irregular time histories to cycles. The algorithm of this technique was borrowed from ASTM E1049 (2017) and input into a computer code to extract the cycle database for 45 years. The simulator software then built structural models for all the wind speeds in the timespan under consideration for each member in the structure, and the stress was extracted at each loading level following the analysis and the number of cycles to failure under this stress level interpolated from the *S-N* curve. The linear damage formula, known as the Palmgren-Miner rule, was used to assess the fatigue condition of each member using Equation 3.5.

$$D_i = \frac{n_i}{N_i}$$

Equation 3.5

Where D_i is the damage in a specific member at a particular stress range, n_i is the number of cycles at *i-th* stress range (obtained from rainflow analysis), and N_i is the number of cycles to failure at the same stress range obtained from Equation 3.4.

After assessing the damage at each stress level resulting from the application of all the wind speeds in the timespan under consideration, the total damage was computed using Equation 3.6.

$$D = \sum_i D_i$$

Equation 3.6

According to the Palmgren-Miner rule, fatigue failure is expected when such life fractions sum to a unity, that is when 100% of the life is exhausted (*D=1).*

3.5.3 Fatigue Life Calculation Automation

This study also built a comprehensive tool to accurately predict the remaining fatigue life of full-span overhead sign support structures subjected to long and sustained wind fluctuation as well as the 45-year wind database histories. The result was a computationally affordable simulation package to evaluate the fatigue life of structural members and detect members that are prone to fatigue failure. Users of the developed software select the city, define the structural geometry, and select the timespan the structure has been in service, such as the year the structure was built and how long the structure has been in service at the time of evaluation (Figure 3.5). The software extracts the wind speeds and the number of cycles for each speed for that timespan from the previously established database. The finite element software Staad Pro (Bentley Systems, 2016) then runs analyses to cover all wind speeds, and the post-processing engine calculates the damage index for each member in the structure using the rules mentioned earlier. Then a color index screen results pops up for the user to identify damaged members.

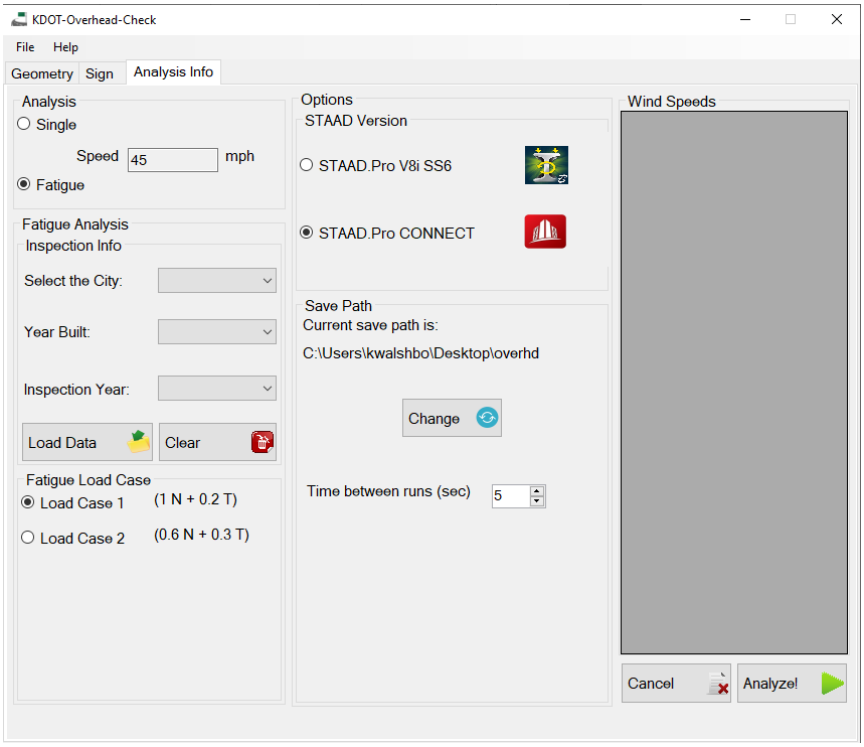

Figure 3.5: Fatigue Life Software Interface

Chapter 4: Results and Discussion

4.1 Results of the Wichita Structure

Figure 4.1 shows this study's methodology to evaluate and assess overhead sign support structures for remaining fatigue life. This procedure yielded a stand-alone software written in the C# programming language. To validate functionality and the software algorithm, it was used as an inspection tool to evaluate a four-chord box overhead truss in Wichita, Kansas. As shown in Figure 4.2, the structure was modeled using the developed model generator and the parameters in Table 4.1. The structure was then exposed to 45 years of wind loading since it was built in 1975 and inspected in 2019. The present methodology and procedure could be followed to produce a similar tool to account for different geometries and wind raw records.

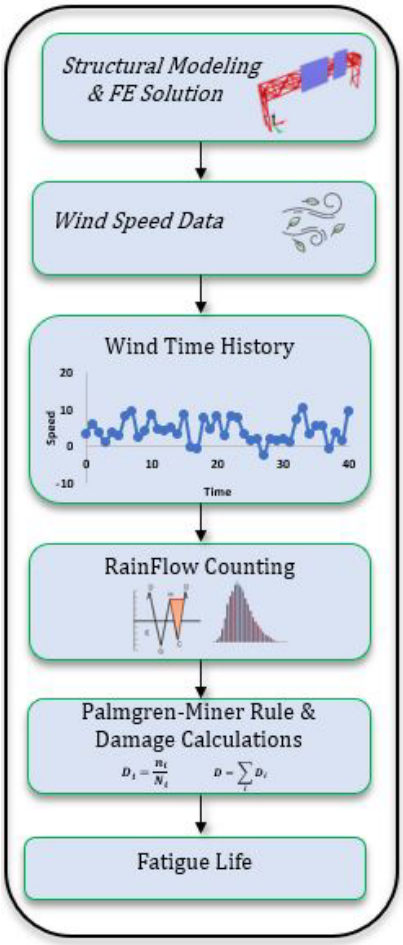

Figure 4.1: Fatigue Life Calculation Flowchart

Table 4.1: Wichita Model Information

Geometry								
Main truss dimension		Right truss dimension		Left truss dimension		Sign information (ft)		
Span	5.87 ft	Span	5.65 ft	Span	5.44 ft		S 1	S 2
Number of panels	12	Number of panels	3	Number of panels	3	Location	22.8	48.2
Main wall thick.	0.148 in	Main wall thick.	0.279 in	Main wall thick.	0.279 in	Height	7.5	8
Secondary wall thick.	0.12 in	Sec. wall thick.	0.12 in	Secondary wall thick.	0.12 in	Width	19.25	11.5

Material (Aluminum)	
Parameter	Value
Young's Modulus	10100 ksi
Poisson's Ratio	0.35
Density	2574.3kg/m^3

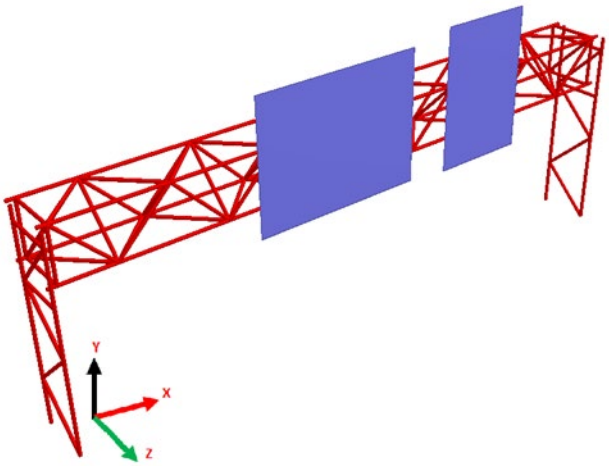

Figure 4.2: Wichita Staad Model

After completing 45 analyses (1–45 mph) via Staad Pro and reading back-sorting the analysis results, the fatigue engine performed calculations to evaluate the fatigue life consumption in all members in the analytical model. Because the model contained 161 members, evaluating the

fatigue life for all members would have been computationally cumbersome without the developed software. When the analysis was complete, the results window indicated the fatigue life for all model members. As shown in Figure 4.3, members 258 and 259 (red) reached the end of their fatigue lives with a damage index of 1.07. Based on the Palmgren-Miner rule, a member reaches the end of its fatigue life when the damage index surpasses unity. Since those two members exceeded a damage index of unity, both members reached their ultimate fatigue failure, leading to an increased tendency to develop visible fatigue cracks. Notably, distressed members 258 and 259 are adjacent to each other; member 260 in their vicinity reflected a damage index of 0.83.

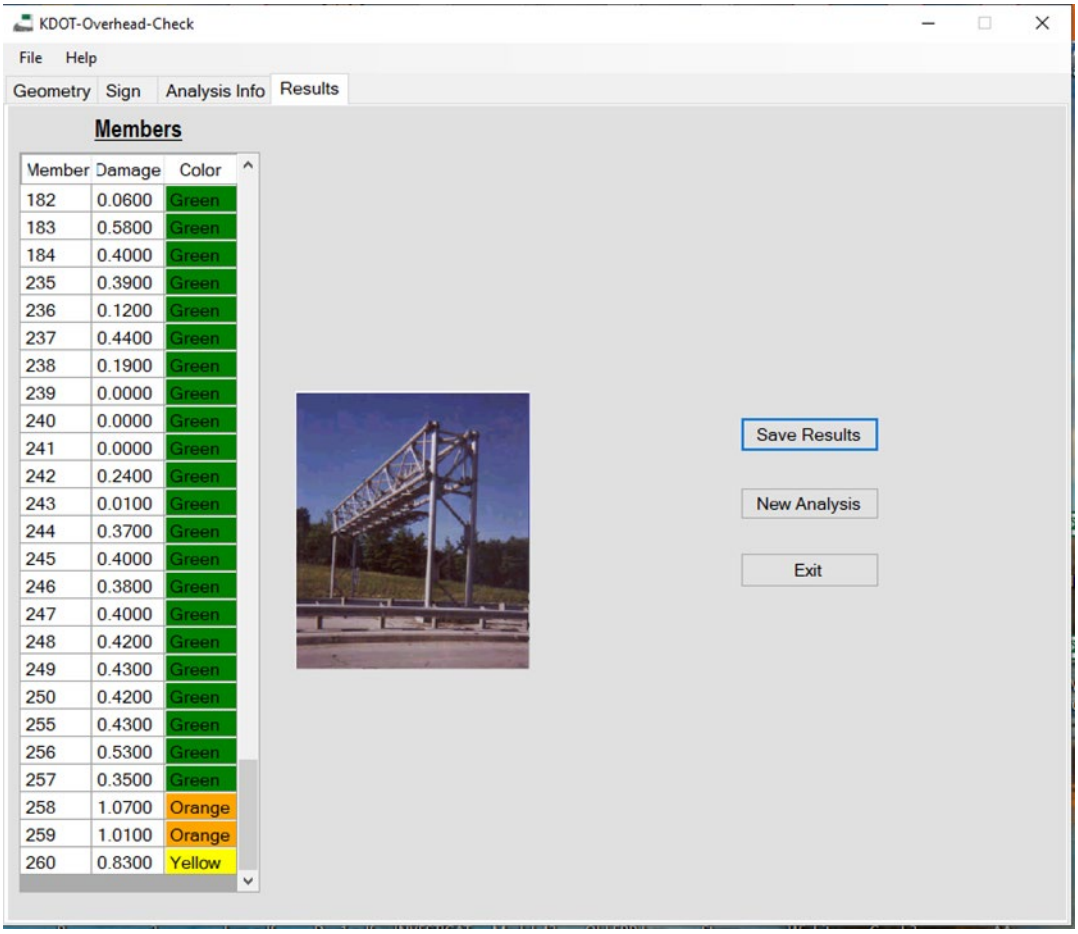

Figure 4.3: Fatigue Life Results Sample for the Wichita Model

4.2 Comparison of Model 1 Results

This study used model 1 (Alshareef et al., 2022) to test, verify, and compare results. Figure 4.4 shows the simulated structural model dimensions for structure members and signs, specifically the horizontal truss span of the structure (70 ft), sign 1 (17 ft 6 in. × 12 ft), sign 2 (15 ft 6 in. × 6 ft 6 in.). Figure 4.5 shows the sign truss interface with all input data necessary to generate model 1. The first sign truss data fields, "S left" and "S right," refer to the vertical node spacing at the two sides' columns. "N" refers to the number of bays in the vertical columns, while "S Horiz" and "N" refer to the node spacings and the number of spans in the horizontal truss, respectively. The horizontal offset from the columns is the distance by which the horizontal truss is shifted from the columns (given as 11.6 in. for model 1).

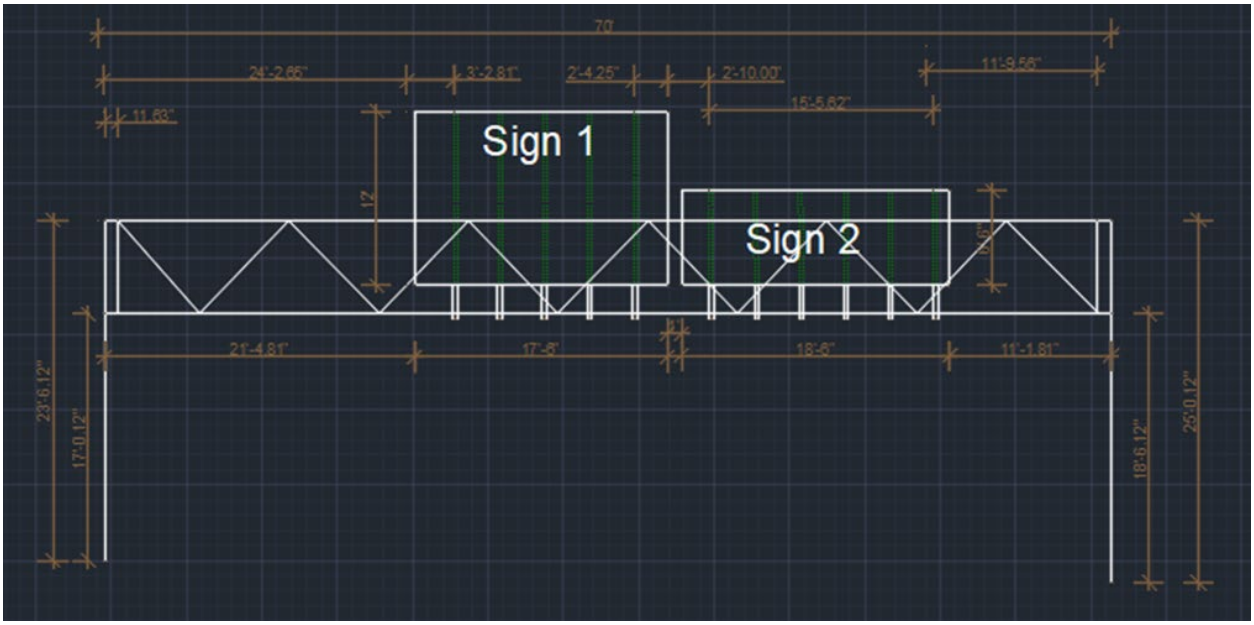

Figure 4.4: Model 1 Structure and Dimensions

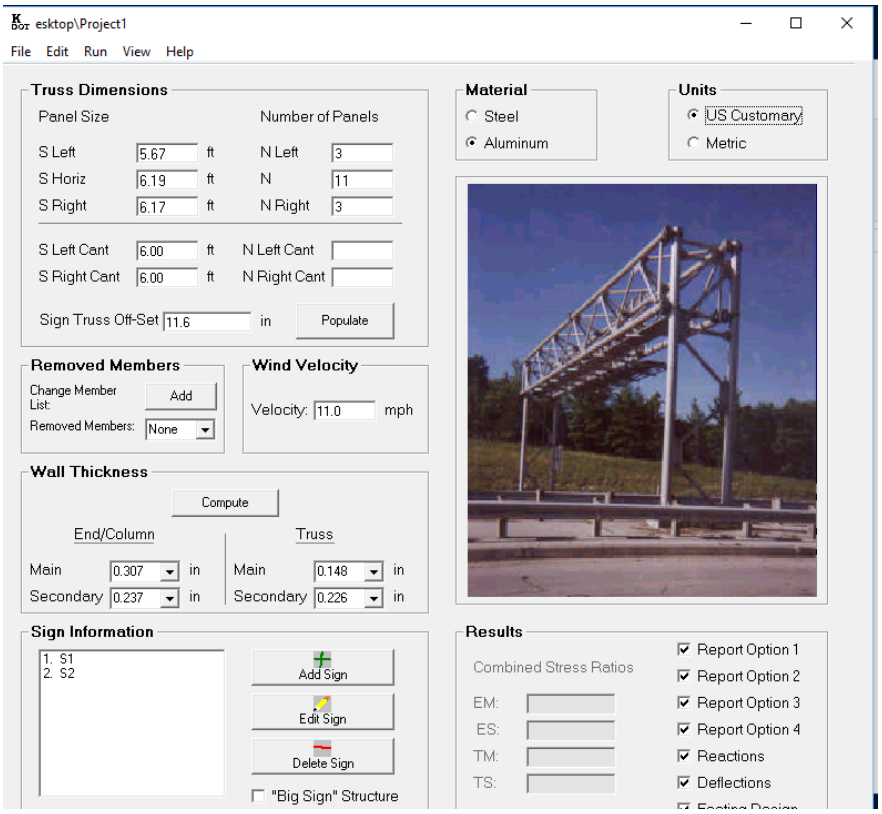

Figure 4.5: KDOT Sign Truss Interface with Model 1 Input Data

The developed software was used to obtain results for Model 1 using wind speed records for the city of Topeka to compare results to the old software, which utilized deterministic wind model fluctuation. Figure 4.6 shows the total damage for selected members from both models. As shown, damage from the 1-Hz model was more significant than damage from the new model for most members, although the models retained a similar trend. For example, the highest damaged member from the 1-Hz model showed the highest damage in the new model. The methodology used in the 1-Hz model calculation assumed very large numbers of wind cycles to account for all possible vibration sources without considering dynamic effects. The old model used stress from the finite element solution, while the new model used the rainflow counting technique to obtain wind speed cycles. A DAF was used to amplify the resulting stress to account for the dynamic nature of wind, which yields higher pseudo stress. Figure 4.7 compares the stress values used in fatigue calculation. Higher stress produced fewer cycles (N) to failure, as evidenced by the S-N curve. For all members at any wind speed, the number of cycles to failure was lower in the new model than the 1-Hz model due to increased pseudo stress.

Conversely, the number of wind speed cycles from the 1-Hz model was significantly higher than in the new model, as shown in Figure 4.8, and the spectrum content of the wind speed for the new model was significantly shorter than the corresponding 1-Hz model. This difference significantly impacts the summed individual damage indices when producing the total damage index for each member. Figure 4.9 shows the number of cycles to failure for selected members at a 15-mph wind speed. Comparison results of these values from both models revealed that the number of cycles from the new model was much lower. Calculations of the fractional damage in the same members for 15 mph yielded a higher damage index from the new model than the 1-Hz model, as shown in Figure 4.10, because the single-speed damage index depends on the ratio between the number of wind cycles to the number of cycles to failure. These results would not apply for other wind speeds, however, since the ratio between the number of cycles to failure (new model) and the number of cycles to failure (1-Hz model) for certain wind speeds is constant, while the ratio of the number of wind cycles (new model) to the number of wind cycles (1-Hz model) may differ for other wind speeds that yield to different damage index trends. This explains why the total damage index for certain members was higher in the old model since the total damage is the sum of the individual single-speed damage index.

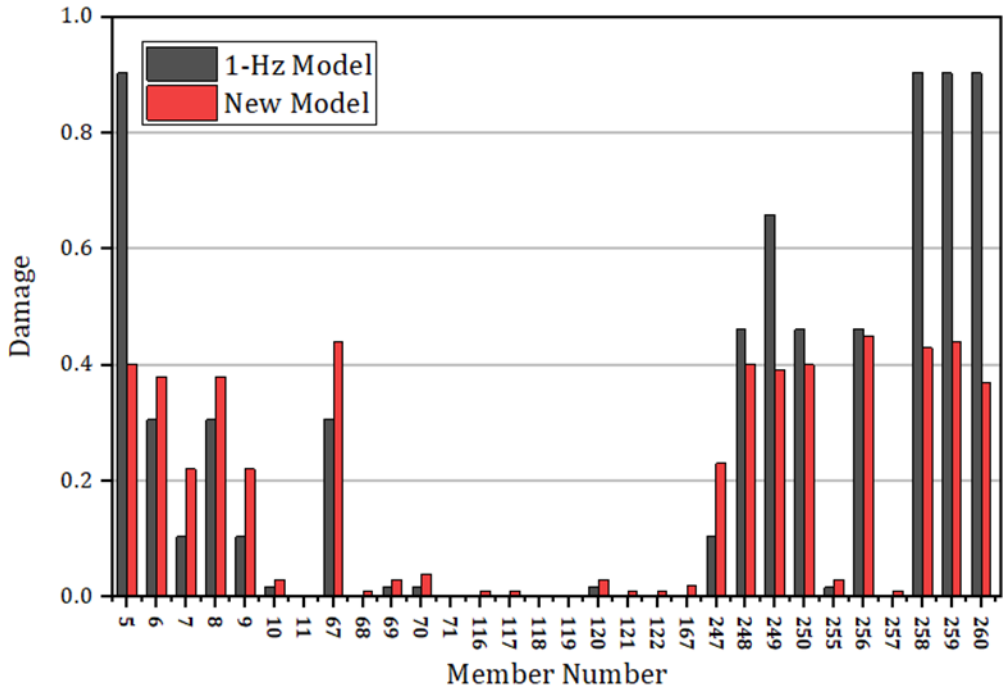

Figure 4.6: Palmgren-Miner Rule Results for Sample Members of Model 1 in Topeka

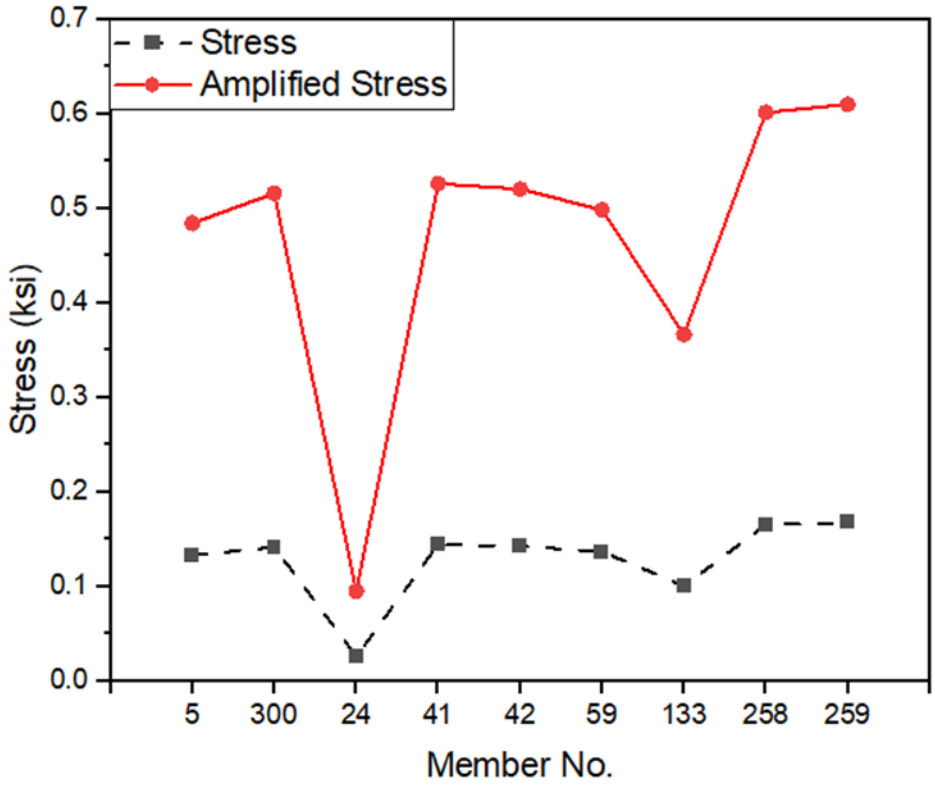

Figure 4.7: Stress versus Amplified Stress for Members at 15 mph Wind Speed

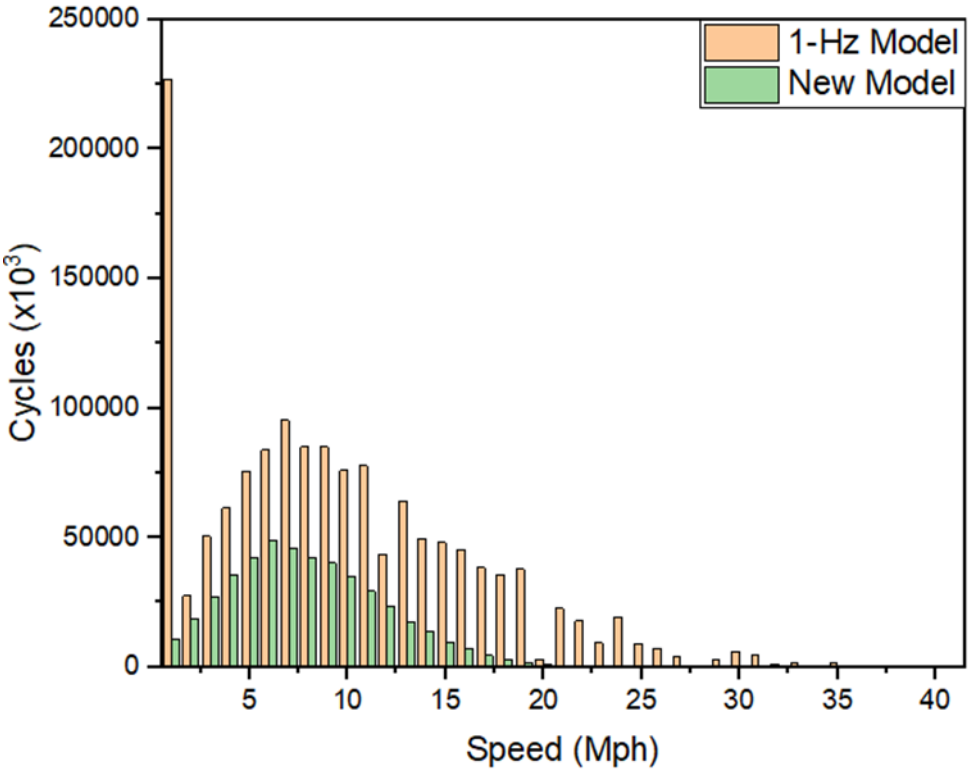

Figure 4.8: Wind Speed versus Number of Cycles

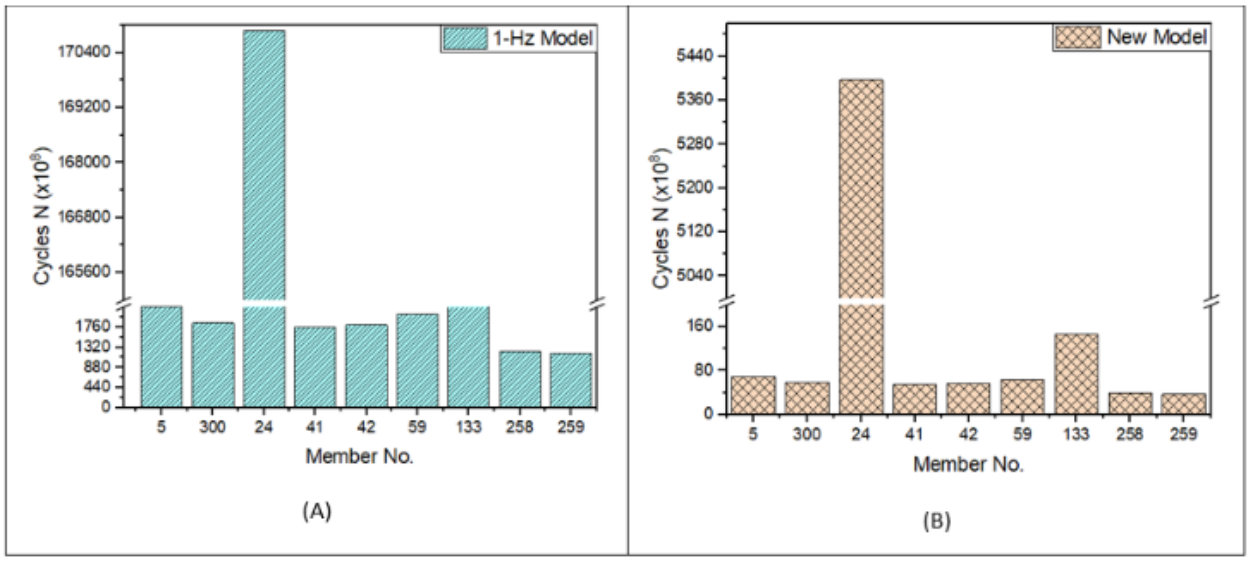

Figure 4.9: Number of Cycles to Failure (*N*) for Members at 15 mph: (A) 1-Hz Model (B) New Model

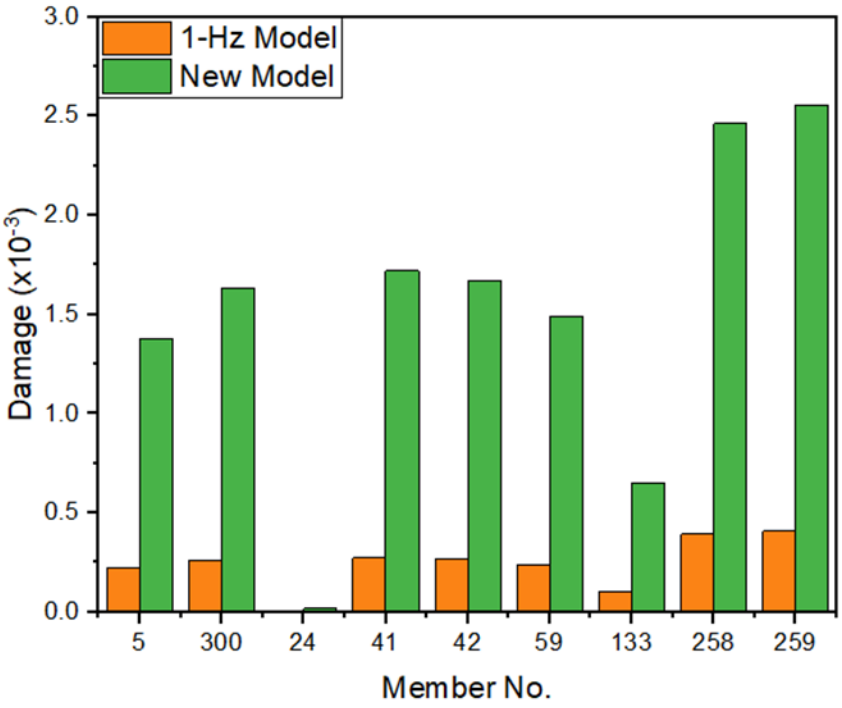

Figure 4.10: Damage in Selected Members at 15 mph

Chapter 5: Conclusions and Recommendations

This study used finite element shape functions to conduct spatial interpolation of wind-speed records for all Kansas counties (Al Shboul et al., 2023). This method considered spatial correlations among boundary sites. Artificial wind-time histories were constructed for each day for the entire 45-year study period, and the number of cycles developed using rainflow analysis was used to provide descriptive wind loading for civil engineering applications. User-friendly software was developed using C# to extrapolate wind-speed cycles for any future year. The following conclusions and findings were drawn from this study:

1. The finite element spatial interpolation technique accurately estimates spatially continuous phenomena from measured values at limited sample points.
2. Adequate care should be given during the meshing of the study area in terms of the element size since this method is highly spatially dependent.
3. The global trend of predicted values in Sedgwick County captured the measured values and continued to commit relatively high peak wind-speed values for the year 1990 and low values in years 2000 and 2005.
4. The number of cycles resulting from the rainflow analysis for the developed time histories was less than the number of cycles previously determined by the deterministic approach at Kansas State University, which was conservatively assumed to include dynamic amplification effects.

References

Al Shboul, K. W., Rasheed, H. A., & AlKhiary, A. (2023) Spatial wind speed interpolation using Isoparametric shape functions for structural loading. *Structures, 50*, 444–463. https://doi.org/10.1016/j.istruc.2023.02.037

Alshareef, H. A., Al Shboul, K. W., Rasheed, H. A., & Abouelleil, A. (2022). Analytical-based application software for estimating remaining fatigue life of non-cantilevered sign structures. *Engineering Structures, 262*, Article 114315. https://doi.org/10.1016/j.engstruct.2022.114315

American Association of State Highway and Transportation Officials. (AASHTO). (2015). *2015 Interim revisions to standard specifications for structural supports for highway signs, luminaires, and traffic signals* (6th ed., 2013).

Arabi, S., Shafei, B., & Phares, B. M. (2018). Fatigue analysis of sign-support structures during transportation under road-induced excitations. *Engineering Structures*, *164*, 305–315. https://doi.org/10.1016/j.engstruct.2018.02.031

ASTM E1049. (2017). *Standard practices for cycle counting in fatigue analysis*. ASTM International. https://doi.org/10.1520/E1049-85R17

Bentley Systems. (2016). Staad Pro V8i SS6 [Computer software]. https://www.bentley.com/software/staad/

Chen, G., Wu, J., Yu, J., Dharani, L. R., & Barker, M. (2001). Fatigue assessment of traffic signal mast arms based on field test data under natural wind gusts. *Transportation Research Record, 1770*, 188–194. https://doi.org/10.3141/1770-24

Cochran, L. (Ed.). (2012). *Wind issues in the design of buildings*. American Society of Civil Engineers. https://doi.org/10.1061/9780784412251

Creamer, B. M., Frank, K. H., & Klingner, R. E. (1979). *Fatigue loading of cantilever sign structures from truck wind gusts* (Report No. FHWA/TX-79/10+209-1F). University of Texas at Austin, Center for Highway Research. https://library.ctr.utexas.edu/digitized/texasarchive/phase2/209-1f-chr.pdf

Davenport, A. G. (1962). The spectrum of horizontal gustiness near the ground in high winds. *Quarterly Journal of the Royal Meteorological Society, 88*(376), 197–198. https://doi.org/https://doi.org/10.1002/qj.49708837618

DeSantis, P. V., & Haig, P. E. (1996). Unanticipated loading causes highway sign failure. In A. Ali et al. (Eds.), *1996 ANSYS Conference proceedings* (Vol. 3, pp. 98–103). ANSYS, Inc.

Dexter, R. J., & Ricker, M. J. (2002). *Fatigue-resistant design of cantilevered signal, sign, and light supports* (NCHRP Report 469). Transportation Research Board. https://onlinepubs.trb.org/onlinepubs/nchrp/nchrp_rpt_469-a.pdf

Fouad, F. H., & Hosch, I. E. (2011). *Design of overhead VMS structures for fatigue loads* (Report No. 09203). University of Alabama, University Transportation Center for Alabama. https://rosap.ntl.bts.gov/view/dot/25439

Ginal, S. (2003). *Fatigue performance of full-span sign support structures considering truck-induced gust and natural wind pressures* (Master's thesis; *Online access restricted to Marquette Campus*). Marquette University. https://epublications.marquette.edu/theses/4785

Hong, H. P., Zu, G. G., & King, J. P. C. (2016). Estimating fatigue design load for overhead steel sign support structures under truck-induced wind pressure. *Canadian Journal of Civil Engineering, 43*(3), 279–286. https://doi.org/10.1139/cjce-2015-0158

Hosch, I. E., & Fouad, F. H. (2010). Design fatigue load of sign support structures due to truck-induced wind gust. *Transportation Research Record*, *2172*, 30–37. https://doi.org/10.3141/2172-04

Kacin, J., Rizzo, P., & Tajari, M. (2010). Fatigue analysis of overhead sign support structures. *Engineering Structures, 32*(6), 1659–1670. https://doi.org/10.1016/j.engstruct.2010.02.014

Kaimal, J. C., Wyngaard, J. C., Izumi, Y., & Coté, O. R. (1972). Spectral characteristics of surface-layer turbulence. *Quarterly Journal of the Royal Meteorological Society, 98*(417), 563–589. https://doi.org/10.1002/qj.49709841707

Letchford, C. J., & Cruzado, H. (2008). *Risk assessment model for wind-induced fatigue failure of cantilever traffic signal structures* (Report No. FHWA/TX-07-4586-4). Texas Tech University, Center for Multidisciplinary Research in Transportation.

Li, X., Whalen, T. M., & Bowman, M. D. (2005). Fatigue strength and evaluation of double-mast arm cantilevered sign structures. *Transportation Research Record*, *1928*, 64–72. https://doi.org/10.1177/0361198105192800107

Matsuishi, M., & Endo, T. (1968). Fatigue of metals subjected to varying stress. *Preliminary proceedings of the Kyushu District Meeting, Fukuoka, March 1968* (Vol. 2, pp. 37–40). Japan Society of Mechanical Engineers.

Sonsino, C. M. (2007). Course of SN-curves especially in the high-cycle fatigue regime with regard to component design and safety. *International Journal of Fatigue, 29*(12), 2246–2258. https://doi.org/10.1016/j.ijfatigue.2006.11.015

AD ASTRA PER ASPERA

Kansas

Department of Transportation